Prolonged Residence Time of a Noncovalent Molecular Adapter, β-Cyclodextrin, within the Lumen of Mutant α-Hemolysin Pores

Li-Qun Gu,[1] Stephen Cheley,[1] and Hagan Bayley[1,2]

[1]Department of Medical Biochemistry and Genetics, The Texas A&M University System Health Science Center, College Station, TX 77843
[2]Department of Chemistry, Texas A&M University, College Station, TX 77843

ABSTRACT Noncovalent molecular adapters, such as cyclodextrins, act as binding sites for channel blockers when lodged in the lumen of the α-hemolysin (αHL) pore, thereby offering a basis for the detection of a variety of organic molecules with αHL as a sensor element. β-Cyclodextrin (βCD) resides in the wild-type αHL pore for several hundred microseconds. The residence time can be extended to several milliseconds by the manipulation of pH and transmembrane potential. Here, we describe mutant homoheptameric αHL pores that are capable of accommodating βCD for tens of seconds. The mutants were obtained by site-directed mutagenesis at position 113, which is a residue that lies near a constriction in the lumen of the transmembrane β barrel, and fall into two classes. Members of the tight-binding class, M113D, M113N, M113V, M113H, M113F and M113Y, bind βCD ~10^4-fold more avidly than the remaining αHL pores, including WT-αHL. The lower K_d values of these mutants are dominated by reduced values of k_{off}. The major effect of the mutations is most likely a remodeling of the binding site for βCD in the vicinity of position 113. In addition, there is a smaller voltage-sensitive component of the binding, which is also affected by the residue at 113 and may result from transport of the neutral βCD molecule by electroosmotic flow. The mutant pores for which the dwell time of βCD is prolonged can serve as improved components for stochastic sensors.

KEY WORDS: α-toxin • molecular adapter • mutagenesis • pore • stochastic sensing

INTRODUCTION

Considerable effort has been spent on the engineering of soluble proteins, such as enzymes and antibodies, both by natural and unnatural amino acid substitution, and by targeted chemical modification. By contrast, the engineering of transmembrane channels and pores is a relatively unexplored area (Bayley, 1999) that is worth examination because membrane proteins differ in environment and structure compared with soluble proteins. Further, just as in the case of soluble proteins, applications for engineered channels and pores are emerging in several areas of biotechnology (Bayley, 1999).

To further efforts in both the protein engineering and the biotechnology of membrane proteins, we have been working with the bacterial pore-forming toxin, staphylococcal α-hemolysin (αHL).* The αHL pore is a heptamer made up of identical subunits of 293 amino acids (see Fig. 1 A). Roughly globular molecules with molecular masses of up to ~2,000 D (Füssle et al., 1981), or larger elongated polymers such as single-stranded nucleic acids (Kasianowicz et al., 1996), can pass through a channel centered on the molecular sevenfold axis of the pore (see Fig. 1 A). Before the crystal structure of the αHL pore was solved (Song et al., 1996), we used biochemical knowledge to engineer triggers and switches into the protein through which the assembly pathway could be controlled by a variety of agents including metal ions, enzymes, and light (Bayley, 1995, 1997). Potential applications of these molecules include the use of metal-regulated pores for reversible cell permeabilization (Russo et al., 1997; Otto-Bruc et al., 1998; Eroglu et al., 2000) and the development of cytotoxic agents activated by cell-surface proteases (Walker and Bayley, 1994; Panchal et al., 1996).

The availability of the structure of the αHL pore (Song et al., 1996) allowed us to focus on the properties of fully assembled pores altered by direct mutagenesis (Braha et al., 1997) or by targeted covalent modification (Movileanu et al., 2000; Howorka et al., 2001a,b). From the viewpoint of biotechnology, the primary goal has been to produce pores that respond to various analytes as components for stochastic sensors operating at the single molecule level (Bayley et al., 2000; Bayley and Cremer, 2001). For example, direct mutagenesis has permitted the detection of divalent metal ions (Braha et al., 1997, 2000), whereas the covalent attachment of ligands has allowed the detection of proteins (Movileanu et al., 2000) and DNA (Howorka et al., 2001a).

The online version of this article contains supplemental material.

Address correspondence to Dr. Hagan Bayley, Department of Medical Biochemistry and Genetics, The Texas A&M University System Health Science Center, 440 Reynolds Medical Building, College Station, TX 77843-1114. Tel.: (979) 845-7047; Fax: (979) 847-9481; E-mail: bayley@tamu.edu

*Abbreviations used in this paper: αHL, staphylococcal α-hemolysin; βCD, β-cyclodextrin.

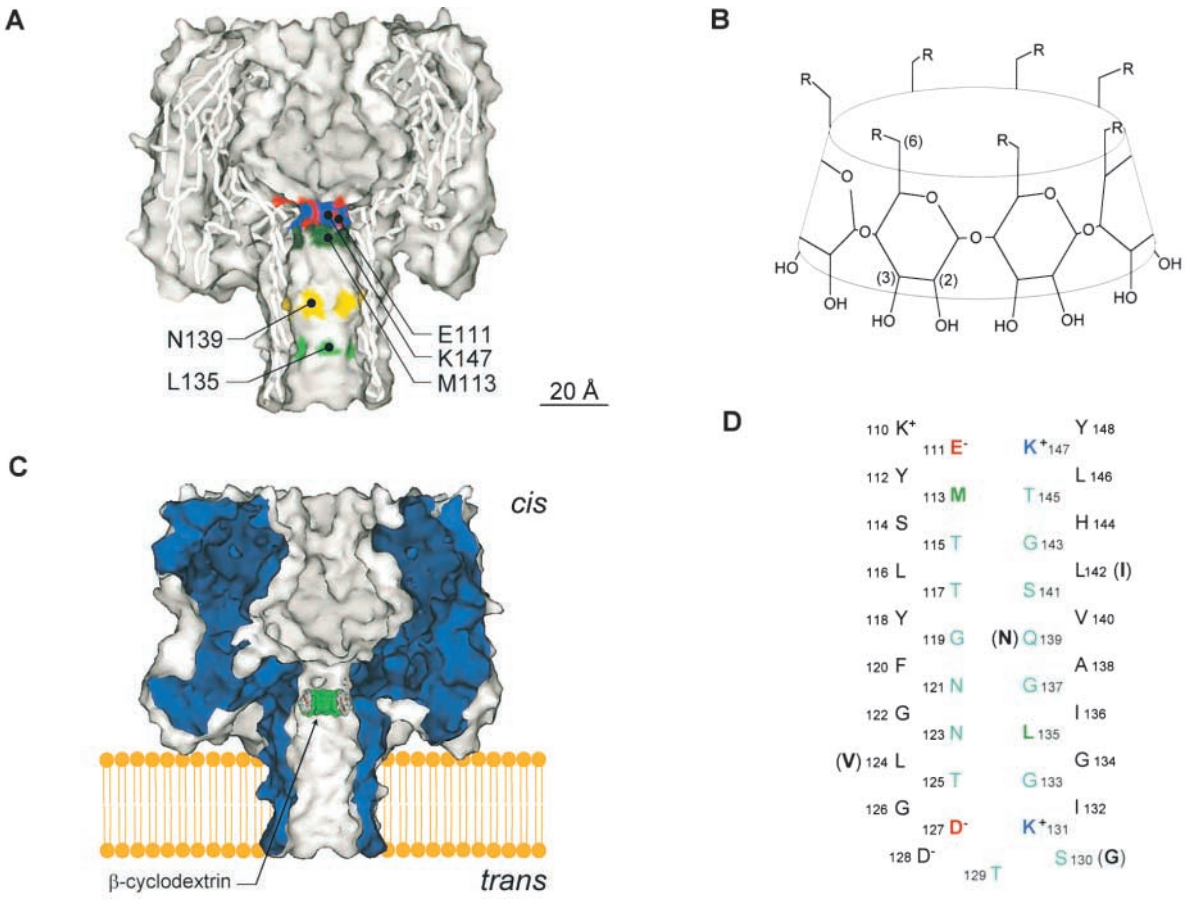

FIGURE 1. Representations of staphylococcal α-hemolysin (αHL) and β-cyclodextrin (βCD). (A) Sagittal section through the WT-αHL pore showing the location of Met-113 (dark green), Glu-111 (red), Lys-147 (blue), Asn-139 (yellow), and Leu-135 (green). (B) Structure of βCD. (C) Schematic of the WT-αHL pore showing βCD lodged in the lumen of the channel. The location is based on mutagenesis data (Gu et al., 1999, 2001), including that described here. (D) Sequence of the transmembrane β barrel of αHL-RL2. WT residues are shown in parentheses.

The stochastic sensing of small organic molecules was a substantial challenge that was solved by the introduction of noncovalent molecular adapters (Fig. 1, B and C; Gu et al., 1999). Adapter molecules, such as cyclodextrins, can become lodged in the lumen of the αHL pore, where they remain available for the host–guest interactions that are well-known to occur in solution (D'Souza and Lipkowitz, 1998). Hence, binding of a cyclodextrin within the lumen of the αHL pore causes a reduction in current flowing through the pore. Additional transient reductions in the current are brought about by the subsequent binding of organic analyte molecules to the cyclodextrin, permitting the analyte to be identified and quantified (Gu et al., 1999). Other molecules, notably cyclic peptides, can act as adapters (Sanchez-Quesada et al., 2000). The adapters can bring about further changes in the properties of the αHL pore; for example, they can alter ion selectivity (Gu et al., 2000; Sanchez-Quesada et al., 2000).

Because of the utility of noncovalent molecular adapters, it is important to maximize their dwell times within the lumen of the pore. The dwell time of β-cyclodextrin (βCD) within the pore can be extended to several milliseconds at low pH and high negative transmembrane potentials or at high pH and high positive potentials (Gu and Bayley, 2000). However, it would be advantageous to lengthen the residency to seconds or longer. We have already shown that the mutant M113N binds βCD with high affinity (Gu et al., 1999) and, recently, this finding was extended when a nanocavity was built between two different cyclodextrins lodged in the transmembrane β barrel (Gu et al., 2001). Met-113 is located near the constriction at the internal end of the β barrel (Fig. 1 A); here, we report in detail the results of mutagenesis of Met-113 to each of the remaining nineteen natural amino acids.

MATERIALS AND METHODS

Mutagenesis of αHL at Position 113

All Met-113 mutants were made by cutting pT7-αHL-RL2 (Cheley et al., 1999) with SacII and HpaI and replacing the excised in-

ternal fragment with duplex DNA formed from 5′-GGAATTCGATTGATACAAAAGAGTAT**xyz**AGTACGTT-3′ (sense) and 5′-AACGTACT**z′y′x′**ATACTCTTTTGTATCAATCGAATTCCGC-3′ (antisense), where **xyz** and **z′y′x′** represent, respectively, the codon and anticodon replacements for the following: Ala (**xyz =** GCA/ **x′y′z′** = TGC), Cys (TGC/GCA), Asp (GAT/ATC), Glu (GAG/CTC), Phe (TTT/AAA), Gly (GGG/CCC), His (CAT/ATG), Ile (ATT/AAT), Lys (AAA/TTT), Leu (CTA/TAG), Asn (AAT/ATT), Pro (CCA/TGG), Gln (CAG/CTG), Arg (AGA/TCT), Ser (AGC/GCT), Thr (ACT/AGT), Val (GTT/AAC), Trp (TGG/CCA), and Tyr (TAT/ATA). Because these changes were made in the RL2 background (Cheley et al., 1999), each mutant contains the following additional replacements with respect to WT-αHL: Lys-8 → Ala, Val-124 → Leu, Gly-130 → Ser, Asn-139 → Gln, and Ile-142 → Leu.

Additional αHL Mutants

Replacements of charged residues near the constriction were also made by constructing the mutants K147N, E111N/K147N, and E111N/M113N/K147N. First, mutants αHL-E111N and αHL-K147N were constructed by cutting pT7-αHL-RL2 with the enzyme pairs SacII-HpaI and AflII-XhoI, respectively, and replacing the excised internal fragments with, respectively, the duplexes formed from 5′-GGAATTCGATTGATACAAAAAATTATATGAGTACGTT-3′ (sense) and 5′-AACGTACTCATATAATTTTTTGTATCAATCGAATTCCGC-3′ (antisense) and from 5′-TTAATTATGTTCAACCTGATTTCAAAACAATTC-3′ (sense) and 5′-TCGAGAATTGTTTTGAAATCAGGTTGAACATAA-3′ (antisense). To construct the double mutant E111N/K147N, pT7-αHL-K147N was digested with HpaI and HindIII, and the resulting internal fragment was inserted into pT7-αHL-E111N that had been cut with the same enzymes. The triple mutant E111N/M113N/K147N was prepared by cutting pT7-αHL-K147N with SacII and HpaI and replacing the small fragment with duplex DNA prepared from 5′-GGAATTCGATTGATACAAAAAATTATAATAGTACGTT-3′ (sense) and 5′-AACGTACTATTATAATTTTTTGTATCAATCGAATTCCGC-3′ (antisense). Because these changes were made in the RL2 background (Cheley et al., 1999), each mutant contained the additional replacements listed above.

Mutants M113N(WT), N139Q(WT), and M113N/N139Q (WT) were constructed as described previously (Gu et al., 2001). αHL-L135N was constructed by cutting pT7-αHL-RL1 (Cheley et al., 1997) with SpeI and ApaI and replacing the fragment with duplex DNA prepared from 5′ CTAGTAAAATTGGAGGCAATATTGGGGCCCAGG-3′ (sense) and 5′ GGCCCCAATATTGCCTCCAATTTTA-3′ (antisense). The StuI site that is present in the αHL-RL1 gene, but absent in αHL-L135N, was used to screen for cassette replacement before DNA sequencing. RL1 encodes the same amino sequence as RL2, but contains different restriction sites. Therefore, in the text, L135N is treated as having the RL2 background. αHL-M113N/L135N was constructed in a similar fashion. pT7-αHL-M113N (RL2 background; see above) was cut with SpeI and ApaI, and the fragment was replaced with duplex DNA prepared from the same oligonucleotides used to construct αHL-L135N (see above). As before, plasmids were screened by digestion with StuI.

DNA Sequencing

The genes of all αHL mutants used in this work were sequenced entirely. Sequencing was performed with SC001 (upstream forward primer) 5′-CACTATAGGGAGACCACAACGG-3′ and SC003 (internal forward primer) 5′-CAGGGTTTTCACCAGACTTCGC-3′. No changes were found, except for those intended.

αHL Homoheptamer Formation and Purification

Heptameric WT-αHL was formed by treating monomeric αHL, purified from *Staphylococcus aureus*, with deoxycholate (Bhakdi et al., 1981; Walker et al., 1992) and isolated from SDS–polyacrylamide gels as described previously (Braha et al., 1997). The remaining αHL polypeptides were synthesized in vitro by coupled transcription and translation (IVTT) and assembled into homoheptamers by the inclusion of rabbit red cell membranes during synthesis, as described previously (Cheley et al., 1999). The heptamers were purified by SDS-PAGE and stored in 50-μl aliquots at −80°C (Cheley et al., 1999). All mutant polypeptides were synthesized and purified twice.

Planar Bilayer Recordings

Planar bilayer recordings were made as described at 22 ± 2°C (Gu and Bayley, 2000; Gu et al., 2000). Buffers for bilayer recording contained 1 M NaCl and 10 mM dibasic sodium phosphate (Sigma-Aldrich), in deionized water (Millipore Corp.), and were titrated to pH 7.5 with aqueous HCl (EMScience). The bilayer was formed from 1,2-diphytanoyl-*sn*-glycero-phosphocholine (Avanti Polar Lipids) over an orifice 50–100 μm in diameter (Montal and Mueller, 1972). The orifice had been pretreated with hexadecane in pentane, and the lipid was transferred to the chambers in pentane. Protein was added to the cis chamber, which was at ground. A positive potential indicates a higher potential in the trans chamber of the apparatus, and a positive current is one in which cations flow from the trans to the cis side. Experiments were initiated by the addition of heptameric αHL to the cis chamber, to a final concentration of 3–30 ng ml^{-1}, with stirring until a single channel appeared. βCD (Sigma-Aldrich) was added to the trans chamber at 40 μM, unless otherwise specified. The amplifier's internal low-pass Bessel filter was set at 5 kHz. Data were acquired at a sampling rate of 20 kHz. The current recordings were analyzed essentially as described previously (Gu and Bayley, 2000; Gu et al., 2000). To determine each set of kinetic constants, three or more experiments had been performed and, in each case, data were analyzed that were acquired for at least 2 min for weak binding mutants (class 2) and at least 1 h for tight binding mutants (class 1). τ_{on} and τ_{off} for βCD for each mutant, for data obtained at either −40 mV or +40 mV and 40 μM βCD, were obtained from dwell-time histograms fitted to single exponentials by the Levenberg-Marquardt procedure. In all cases, the coefficient of determination of the fits was $R \geq 0.85$. The data were replotted in semilogarithmic form for display in the paper. Separate segments of the data yielded similar τ values, suggesting that stationary kinetics prevailed. Kinetic constants were calculated by using $k_{off} = 1/\tau_{off}$, $k_{on} = 1/\tau_{on}[\beta CD]$, and $K_d = k_{off} / k_{on}$, where [βCD] is the concentration of βCD. Values for unitary conductance, k_{on} and k_{off}, and K_d are quoted as the mean ± SD. Ion selectivity (P_{K+}/P_{Cl-}) was determined from reversal potentials measured with the following solution: cis 1,000 mM KCl, 10 mM potassium phosphate, pH 7.5 (dibasic salt titrated with HCl), trans 200 mM KCl, and 10 mM potassium phosphate, pH 7.5 (Gu et al., 2000).

Online Supplemental Material

Supplemental figures are available at http://www.jgp.org/cgi/content/full/118/5/481/DC1. They show examples of dwell-time histograms used to obtain values of τ_{on} for M113E, M113K, M113N, and M113W. The figures also display histograms obtained from independent segments of the recordings to show that the channel kinetics were stationary.

TABLE I

Conductance Values and Kinetic Parameters for the Interaction of βCD with WT-αHL and Met-113 Mutants[a]

αHL pore	Side chain[b]	−40 mV					+40 mV				
		g_P	g_{PC}	k_{on}	k_{off}	K_d	g_P	g_{PC}	k_{on}	k_{off}	K_d
		pS	*pS*	$M^{-1}s^{-1}$	s^{-1}	*M*	*pS*	*pS*	$M^{-1}s^{-1}$	s^{-1}	*M*
WT-αHL	N	651 ± 4	240 ± 3	$4.0 \pm 0.3 \times 10^5$	$1.3 \pm 0.1 \times 10^3$	$3.4 \pm 0.4 \times 10^{-3}$	721 ± 6	253 ± 4	$2.8 \pm 0.2 \times 10^5$	$2.1 \pm 0.2 \times 10^3$	$7.8 \pm 0.3 \times 10^{-3}$
RL-2	N	691 ± 4	255 ± 6	$2.9 \pm 0.1 \times 10^5$	$9.8 \pm 0.3 \times 10^2$	$3.3 \pm 0.2 \times 10^{-3}$	739 ± 7	220 ± 7	$2.4 \pm 0.3 \times 10^5$	$1.5 \pm 0.2 \times 10^3$	$6.9 \pm 0.1 \times 10^{-3}$
M113K	+	558 ± 10	241 ± 3	$3.3 \pm 0.3 \times 10^5$	$7.0 \pm 0.5 \times 10^2$	$2.1 \pm 0.1 \times 10^{-3}$	629 ± 8	181 ± 5	$1.6 \pm 0.2 \times 10^5$	$2.0 \pm 0.1 \times 10^3$	$1.4 \pm 0.1 \times 10^{-2}$
M113R	+	585 ± 6	289 ± 4	$4.3 \pm 0.1 \times 10^5$	$6.6 \pm 0.2 \times 10^2$	$1.6 \pm 0.1 \times 10^{-3}$	666 ± 8	266 ± 3	$2.2 \pm 0.2 \times 10^5$	$3.1 \pm 0.3 \times 10^3$	$1.3 \pm 0.1 \times 10^{-2}$
M113H	+	596 ± 7	193 ± 2	$3.0 \pm 0.6 \times 10^5$	$2.1 \pm 0.4 \times 10^{-1}$	$7.0 \pm 1.7 \times 10^{-7}$	677 ± 4	189 ± 5	$3.3 \pm 0.4 \times 10^5$	$1.1 \pm 0.3 \times 10^{-1}$	$3.0 \pm 1.0 \times 10^{-7}$
M113E	−	743 ± 6	217 ± 3	$1.1 \pm 0.2 \times 10^5$	$1.4 \pm 0.1 \times 10^3$	$1.2 \pm 0.2 \times 10^{-2}$	628 ± 7	153 ± 5	$4.0 \pm 0.3 \times 10^5$	$1.4 \pm 0.1 \times 10^3$	$3.3 \pm 0.5 \times 10^{-3}$
M113D	−	717 ± 3	228 ± 6	$2.9 \pm 0.4 \times 10^5$	$4.9 \pm 1.0 \times 10^{-2}$	$1.7 \pm 0.8 \times 10^{-7}$	662 ± 3	211 ± 6	$3.7 \pm 0.7 \times 10^5$	$4.1 \pm 1.0 \times 10^{-2}$	$1.2 \pm 0.4 \times 10^{-7}$
M113G	P	689 ± 5	252 ± 5	$2.3 \pm 0.1 \times 10^5$	$8.9 \pm 0.8 \times 10^2$	$3.7 \pm 0.3 \times 10^{-3}$	736 ± 9	214 ± 7	$2.3 \pm 0.1 \times 10^5$	$2.0 \pm 0.2 \times 10^3$	$8.4 \pm 1.7 \times 10^{-3}$
M113N	P	632 ± 7	311 ± 3	$2.7 \pm 0.6 \times 10^5$	$3.8 \pm 1.1 \times 10^{-2}$	$1.3 \pm 0.6 \times 10^{-7}$	646 ± 7	297 ± 4	$2.9 \pm 0.6 \times 10^5$	$5.0 \pm 0.8 \times 10^{-2}$	$1.8 \pm 0.8 \times 10^{-7}$
M113Q	P	714 ± 11	242 ± 6	$3.2 \pm 0.2 \times 10^5$	$1.2 \pm 0.1 \times 10^3$	$4.2 \pm 0.2 \times 10^{-3}$	769 ± 10	218 ± 3	$3.2 \pm 0.2 \times 10^5$	$1.6 \pm 0.2 \times 10^3$	$5.1 \pm 0.8 \times 10^{-3}$
M113C	P	576 ± 7	231 ± 5	$2.6 \pm 0.2 \times 10^5$	$1.2 \pm 0.1 \times 10^3$	$4.3 \pm 0.2 \times 10^{-3}$	651 ± 3	199 ± 6	$2.0 \pm 0.2 \times 10^5$	$2.7 \pm 0.1 \times 10^3$	$1.3 \pm 0.2 \times 10^{-2}$
M113S	P	744 ± 6	264 ± 3	$2.5 \pm 0.2 \times 10^5$	$8.0 \pm 0.7 \times 10^2$	$3.4 \pm 0.4 \times 10^{-3}$	761 ± 9	242 ± 4	$1.8 \pm 0.2 \times 10^5$	$1.5 \pm 0.1 \times 10^3$	$8.1 \pm 0.6 \times 10^{-3}$
M113T	P	705 ± 9	241 ± 4	$1.8 \pm 0.2 \times 10^5$	$8.5 \pm 0.9 \times 10^2$	$5.0 \pm 0.6 \times 10^{-3}$	761 ± 5	195 ± 3	$2.3 \pm 0.2 \times 10^5$	$7.5 \pm 0.5 \times 10^2$	$3.0 \pm 0.5 \times 10^{-3}$
M113Y	P	682 ± 6	209 ± 5	$1.8 \pm 0.5 \times 10^5$	$3.2 \pm 0.9 \times 10^{-2}$	$1.9 \pm 0.9 \times 10^{-7}$	698 ± 12	235 ± 8	$2.0 \pm 0.4 \times 10^5$	$3.5 \pm 0.6 \times 10^{-2}$	$1.7 \pm 0.8 \times 10^{-7}$
M113A	N	658 ± 8	243 ± 5	$2.3 \pm 0.2 \times 10^5$	$7.7 \pm 0.4 \times 10^2$	$3.5 \pm 0.3 \times 10^{-3}$	721 ± 9	209 ± 5	$2.3 \pm 0.2 \times 10^5$	$1.5 \pm 0.1 \times 10^3$	$6.0 \pm 0.6 \times 10^{-3}$
M113V	N	722 ± 7	183 ± 7	$2.3 \pm 0.3 \times 10^5$	$6.3 \pm 0.7 \times 10^{-1}$	$2.8 \pm 0.3 \times 10^{-6}$	786 ± 7	202 ± 7	$2.4 \pm 0.2 \times 10^5$	$3.0 \pm 0.2 \times 10^{-1}$	$1.2 \pm 0.3 \times 10^{-6}$
M113L	N	666 ± 7	243 ± 3	$2.7 \pm 0.2 \times 10^5$	$9.5 \pm 0.7 \times 10^2$	$3.8 \pm 0.2 \times 10^{-3}$	763 ± 4	237 ± 5	$2.2 \pm 0.2 \times 10^5$	$1.6 \pm 0.2 \times 10^3$	$7.3 \pm 0.9 \times 10^{-3}$
M113I	N	637 ± 5	232 ± 5	$1.4 \pm 0.1 \times 10^5$	$3.0 \pm 0.1 \times 10^2$	$2.1 \pm 0.1 \times 10^{-3}$	773 ± 6	273 ± 4	$1.4 \pm 0.1 \times 10^5$	$2.6 \pm 0.3 \times 10^2$	$1.7 \pm 0.4 \times 10^{-3}$
M113P	N	816 ± 10	285 ± 4	$2.1 \pm 0.2 \times 10^5$	$1.7 \pm 0.1 \times 10^2$	$8.4 \pm 0.5 \times 10^{-4}$	849 ± 8	246 ± 7	$3.5 \pm 0.2 \times 10^5$	$1.1 \pm 0.1 \times 10^2$	$2.9 \pm 0.3 \times 10^{-4}$
M113F	N	624 ± 4	165 ± 2	$3.1 \pm 0.2 \times 10^5$	$4.0 \pm 0.7 \times 10^{-2}$	$1.2 \pm 0.2 \times 10^{-7}$	702 ± 5	204 ± 5	$1.7 \pm 0.3 \times 10^5$	$8.6 \pm 1.2 \times 10^{-2}$	$5.4 \pm 0.2 \times 10^{-7}$
M113W	N	524 ± 5	165 ± 5	$4.2 \pm 0.4 \times 10^5$	$1.5 \pm 0.1 \times 10^1$	$3.6 \pm 0.3 \times 10^{-5}$	630 ± 7	192 ± 3	$2.1 \pm 0.3 \times 10^5$	$2.0 \pm 0.1 \times 10^1$	$9.7 \pm 2.1 \times 10^{-5}$

[a]1 M NaCl, 10 mM sodium phosphate, pH 7.5, in both the cis and trans chambers. g_P, conductance of the unoccupied αHL pore; g_{PC}, conductance of the occupied pore, αHL•βCD.

[b]Side chain attributes: +, positively charged; −, negatively charged; P, polar; and N, nonpolar.

RESULTS

The WT-αHL Pore and αHL-RL2, with the Background Used for Mutagenesis, Have Similar Properties

The Met-113 replacements examined in this work were made in αHL-RL2. RL2 is the product of a semisynthetic gene that was originally devised to permit ready cassette mutagenesis of the sequence encoding the transmembrane β barrel. RL2, and the mutants described here, contain the following additional mutations over WT-αHL: Lys-8 → Ala, Val-124 → Leu, Gly-130 → Ser, Asn-139 → Gln, and Ile-142 → Leu (Fig. 1 D). Therefore, the properties of the WT and RL2 αHL pores were first compared. They were found to be similar in terms of unitary conductance values and rectification ratios (g_{+40mV}/g_{-40mV}; Table I), but their properties do differ in detail. For example, the extent of channel block by βCD at +40 mV is lower for RL2 (30% residual current) than for WT-αHL (35% residual current), and whereas WT-αHL•βCD is incompletely blocked by a variety of organic molecules (e.g., adamantane-1-carboxylic acid; Gu et al., 1999), RL2•βCD is almost completely blocked by the same molecules (unpublished data).

βCD Exhibits a Prolonged Dwell Time within the Lumen of Certain Met-113 Replacement Mutants

The interaction of βCD was tested with pores formed from 20 αHL polypeptides, representing Met and all 19 natural amino acid substitutions at position 113. As documented above, the mutations were made in the "RL2" background. In single-channel recordings, in all 20 cases, the addition of 40 μM βCD to the trans compartment produced reversible partial blockades of the ionic current (Fig. 2). The dwell times for βCD in the lumen of the pore (τ_{off}, level 2) were strikingly prolonged for certain mutants (Figs. 2 and 3 A), whereas the dwell times for the unoccupied state of each mutant (inter-event interval, τ_{on}, level 1) did not vary as much and are similar to τ_{on} values for βCD and WT-αHL (Fig. 3 A).

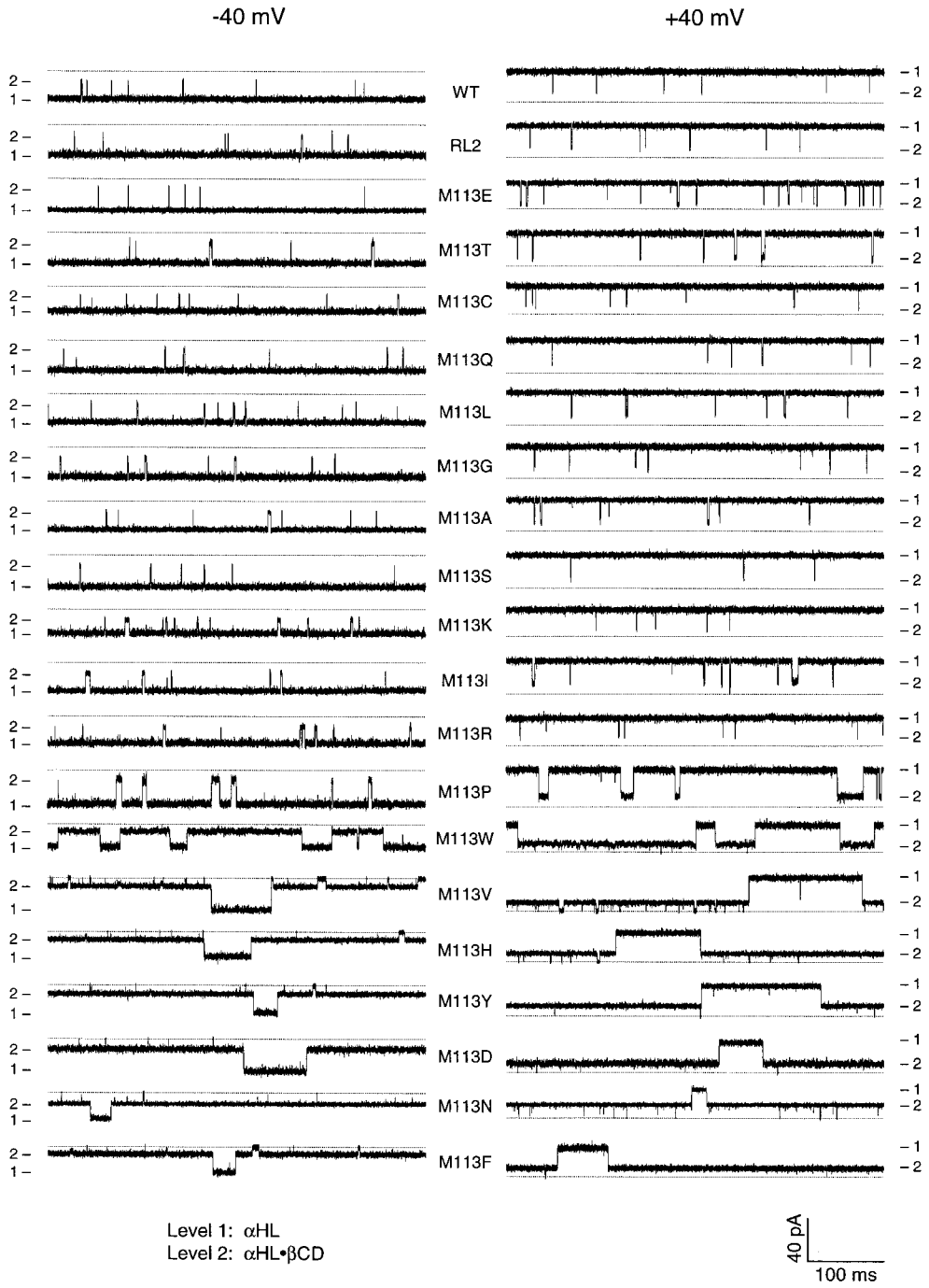

FIGURE 2. Representative current traces from single αHL pores showing the blockade of Met-113 mutants by βCD. All traces were recorded under symmetrical conditions in buffer containing 1 M NaCl, 10 mM sodium phosphate, pH 7.5; 40 μM βCD was added to the trans chamber. (left) Traces recorded at −40 mV; (right) traces recorded at +40 mV. The mutants shown are all derived from RL2 (see the first paragraph of RESULTS). The broken line indicates zero current. The mutants are ordered (top to bottom) according to increasing affinity for βCD.

Interestingly, most of the pores tested could be grouped into two classes according to their τ_{off} values. βCD binds to mutant pores of class 1, namely M113D, M113N, M113V, M113H, M113F, and M113Y, with extended dwell times (τ_{off}) compared with WT-αHL (Fig. 3 A). For example at −40 mV, the dwell time of M113N•βCD (τ_{off} = 27 s) is over 10^4-fold longer than that of WT-αHL•βCD (τ_{off} = 0.76 ms) or RL2•βCD (τ_{off} = 1.0 ms). By contrast, βCD binds to the mutants in class 2 (all but two of the mutants not in class 1) with a dwell time similar to that of WT-αHL or RL2. For example at −40 mV, the dwell time for M113K•βCD is τ_{off} = 1.4 ms. M113W and M113P are borderline cases and were not included in class 1 or 2.

In contrast to τ_{off}, the τ_{on} values of the mutants do not vary greatly and are similar to WT-αHL. For example at −40 mV, the inter-event interval for M113N at 40 μM βCD (τ_{on} = 91 ms) is comparable to that of WT-αHL (τ_{on} = 68 ms) or RL2 (τ_{on} = 93 ms). Therefore, the mutants in class 1, with prolonged τ_{off} values, show high affinity for βCD, whereas mutants in class 2, with short τ_{off} values, show a similar affinity for βCD to WT-αHL (Fig. 2

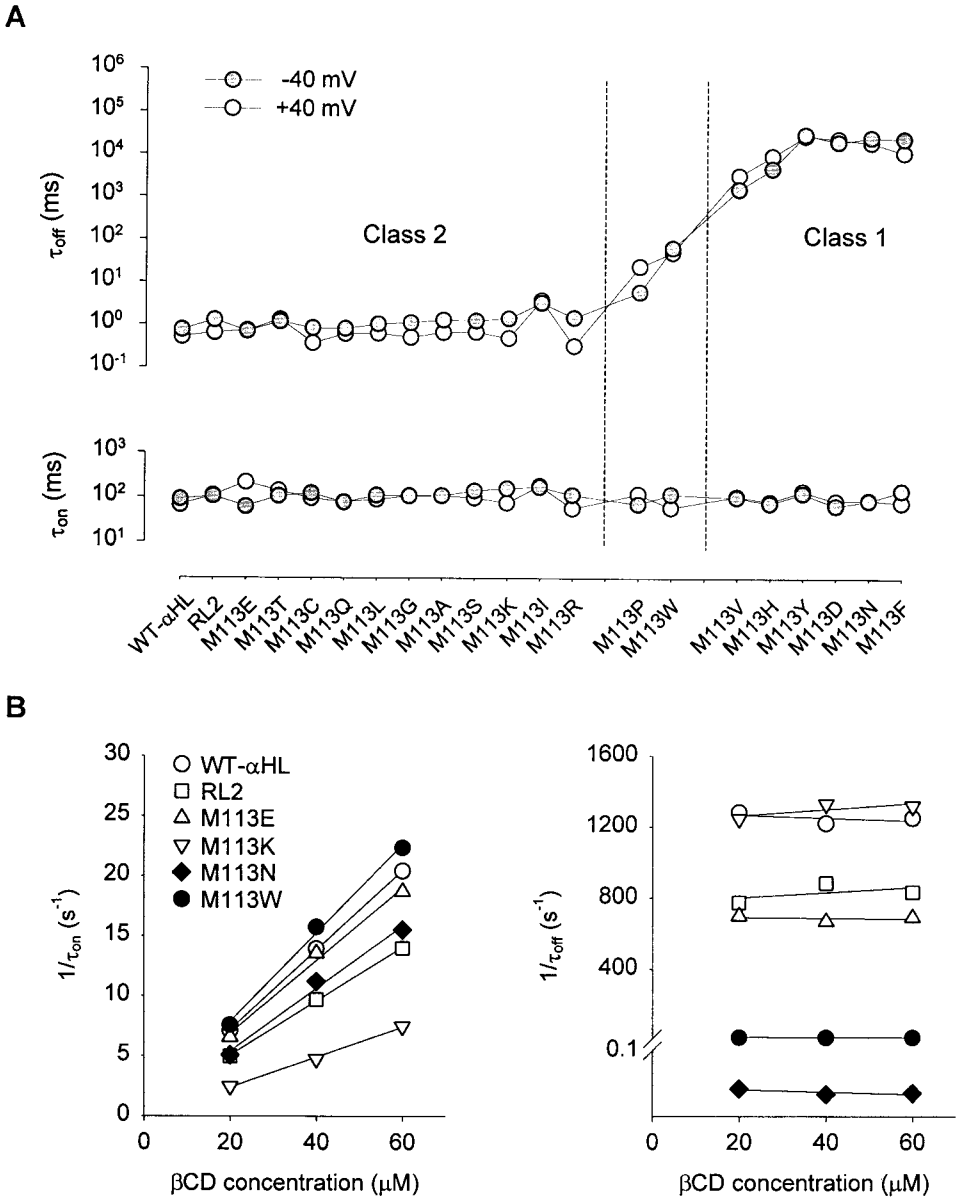

FIGURE 3. Dwell times for the interaction between βCD and the Met-113 mutants. (A) Values of τ_{off}, the dwell time of βCD in the pore, and τ_{on}, the inter-event interval at 40 μM trans βCD. (closed gray circle) −40 mV; (○) +40 mV. The mutants are ordered (left to right) according to increasing affinity for βCD. (B) Dependence of τ_{off} and τ_{on} on the concentration of βCD (trans) for WT-αHL and selected mutants.

and Table I). For example at −40 mV, M113N in class 1 ($K_d = 1.3 \pm 0.6 \times 10^{-7}$ M) binds βCD over 10^4-fold more tightly than WT-αHL ($K_d = 3.4 \pm 0.4 \times 10^{-3}$ M) and RL2 ($K_d = 3.3 \pm 0.2 \times 10^{-3}$ M), whereas M113K in class 2 ($K_d = 2.1 \pm 0.10^{-3}$ M) is similar to WT-αHL in affinity.

βCD Binds to αHL Pores in a Simple Bimolecular Interaction

Level 2 is the only major current blockade level seen in the amplitude histograms of all 20 mutants, which suggests that there is only one major binding site for βCD within the lumen of each αHL pore (Gu and Bayley, 2000). The binding kinetics are also in keeping with this interpretation. As in the case of WT-αHL (Gu and Bayley, 2000), τ_{on} and τ_{off} for βCD for each mutant could be fitted by single-exponential distributions for data obtained at either −40 or +40 mV (1 M NaCl and 10 mM sodium phosphate, pH 7.5) and 40 μM βCD in the trans chamber (*Supplemental Material*). Therefore, the kinetics of the interaction between βCD and the mutant αHL pores most likely obey the simple Scheme I, with $k_{off} = 1/\tau_{off}$, $k_{on} = 1/\tau_{on}[\beta CD]$, and $K_d = k_{off}/k_{on}$, where [βCD] is the concentration of βCD. The kinetic constants were calculated accordingly (Table I).

$$\alpha HL + \beta CD \underset{k_{off}}{\overset{k_{on}}{\rightleftharpoons}} \alpha HL{\bullet}\beta CD$$

(SCHEME I)

In selected cases, WT-αHL, RL2, M113E, M113K, M113N and M113W, the concentration dependence of $1/\tau_{on}$ was examined and found to be proportional to [βCD] (Fig. 3 B), in further support of a simple bimolecular interaction between the pores and βCD.

For mutants in class 1, short additional blockades could be seen while βCD was bound at either −40 or +40 mV. Because their frequency of occurrence was independent of βCD concentration (tested for M113N and M113D; unpublished data), these events are probably not due to the binding of a second βCD. Instead, they may correspond to a second conformation of the occupied state, αHL•βCD. Because, these events occupied <3% of the total βCD binding time, they were merged with level 2 for the kinetic analysis.

βCD Affinity and Side Chain Properties at Position 113

The properties of the side chains at position 113 in the tight-binding class 1 mutants show no obvious relationship with one other. For example, when $1/K_d$, k_{on} and k_{off} are plotted versus side-chain van der Waals volume no pattern is seen, although this is a convenient way to display the data (Fig. 4). Patterns are revealed when the data are examined in detail. Small side chains of <85 Å^3 fall into class 2. Whereas M113N and M113D fall into class 1, mutants with homologous substitution, M113Q and M113E, are in class 2. Similarly, of mutants with nonaromatic hydrophobic amino acid substituents, the one with the lowest volume side chain, M113V, is in class 1, whereas the others M113L, M113I, and RL2 itself (Met-113) are in class 2. Mutants with aromatic substitutions fall into class 1, with the exception of the mutant with the bulkiest substituent, M113W, which has a K_d value intermediate between those characteristic of the two classes.

Single-channel conductance values also show no clear correlation with side-chain van der Waals volume (Fig. 5, A and B, and Table I). Although the presence of seven copies of the bulkiest residue, Trp, at position 113 does yield the pore with the lowest conductance, the effect is not dramatic. The rectification ratios

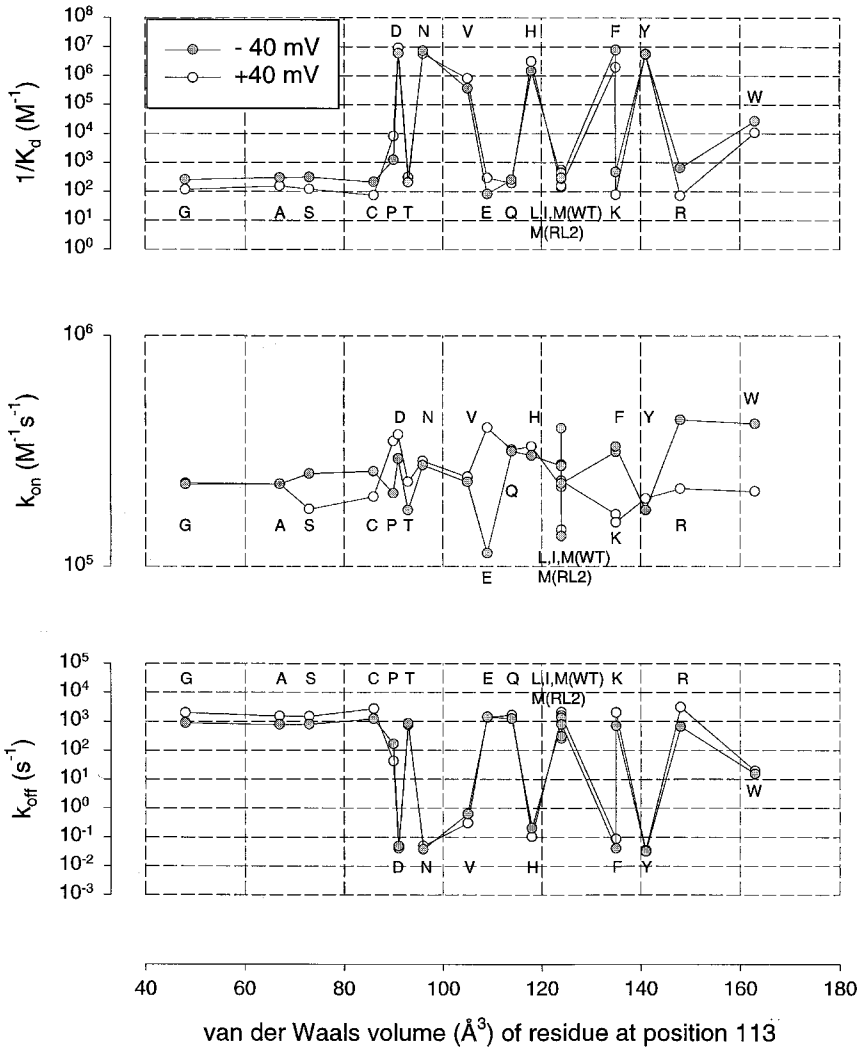

FIGURE 4. Plots of kinetic constants for the Met-113 mutants versus the van der Waals volume (Creighton, 1993) of the residue at position 113. (A) $1/K_d$; (B) k_{on}; and (C) k_{off}. (closed gray circle) −40 mV; (○) +40 mV. Some of the points are obscured, but the values can be found in Table I.

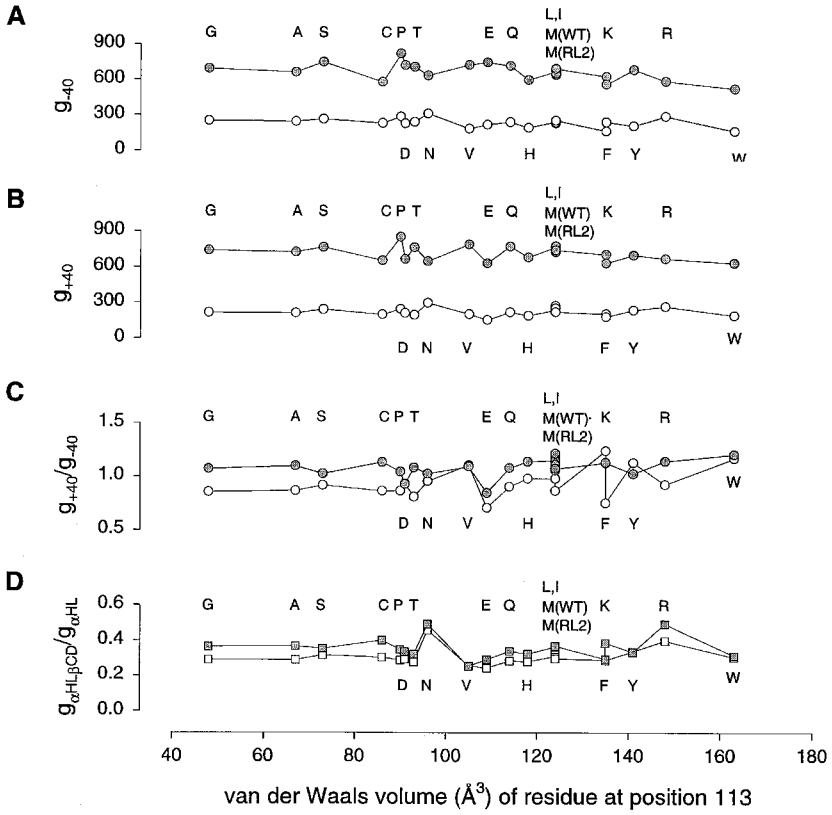

FIGURE 5. Plots of single-channel conductance values for the Met-113 mutants with and without βCD bound versus the van der Waals volume of the residue at position 113. (A) Conductance values at −40 mV: (closed gray circle), αHL conductance; (○) αHL•βCD conductance. (B) Conductance values at +40 mV. (C) Ratio of conductance at +40 mV to conductance at −40 mV (g_{+40}/g_{-40}). (D) Conductance of the pore with βCD bound divided by the conductance of the pore itself. (closed gray square), −40 mV; (□) +40 mV.

($g_{+40\ mV}/g_{-40\ mV}$) also appear to be independent of the van der Waals volume (Fig. 5 C). The extent of block by βCD (Fig. 5 A, B, and D, and Table I) and the rectification ratios with βCD bound (Fig. 5 C) are also uncorrelated with van der Waals volume. There is also no correlation between the examined electrical properties and whether a mutant is a member of class 1 or class 2.

The Interaction of βCD with Pores Mutated at Position 113 Is Independent of Various Other Mutations in the β Barrel

To check the effect of additional mutations in the β barrel on the affinity of βCD, five additional mutants were tested: M113N(WT), N139Q(WT), M113N/N139Q(WT), L135N(RL2), and M113N/L135N(RL2) (Fig. 6). As noted earlier, mutants with the RL2 background contain the following additional mutations over WT-αHL: Lys-8 → Ala, Val-124 → Leu, Gly-130 → Ser, Asn-139 → Gln, and Ile-142 → Leu.

WT-αHL, N139Q(WT), and L135N(RL2) share the residue Met-113, and all three mutants bind βCD weakly: WT-αHL, $K_d = 3.4 \times 10^{-3}$ M; N139Q(WT), $K_d = 2.9 \times 10^{-3}$ M; and L135N(RL2), $K_d = 3.9 \times 10^{-3}$ M. By contrast, M113N(WT), M113N/N139Q(WT) (also named P_{NQ}; Gu et al., 2001) and M113N/L135N(RL2) share Asn at position 113, and all three bind βCD strongly: M113N(WT), $K_d = 2.1 \times 10^{-7}$ M; M113N/N139Q(WT), $K_d = 3.1 \times 10^{-7}$ M; and M113N/L135N(RL2), $K_d = 9.3 \times 10^{-7}$ M. Therefore, the affinity of the αHL pore for βCD is dependent on the residue at position 113, but independent of other sites, notably positions 135 and 139, at least for the substitutions examined here. Residues 135 and 139 project into the lumen of the pore (Fig. 1) and we have previously shown that the mutation N139Q forms a binding site for a different cyclodextrin, hepta-6-sulfato-βCD, but not for βCD (Gu et al., 2001).

A similar pattern was observed when the extent of current block by βCD was examined for the same mutants. βCD reduced the conductance of WT-αHL from 651 to 240 pA (37% residual current), N139Q(WT) from 635 to 253 pA (40%), and L135N(RL2) from 640 to 243 pA (38%). In contrast, the residual conductance values for the pores containing the M113N mutation were as follows: M113N(WT) from 623 to 283 pA with βCD (46%); M113N/N139Q(WT) from 668 to 285 pA (43%); and M113N/L135N(RL2) from 645 to 283 pA (45%). Therefore, the extent of current block by βCD is more dependent on the amino acid at position 113 than those at positions 135 and 139.

The Voltage Dependence of βCD Binding Is Correlated with the Charge Selectivity of the Mutant Pores

The affinity of each mutant αHL pore for βCD is voltage dependent. βCD binds to some mutants more

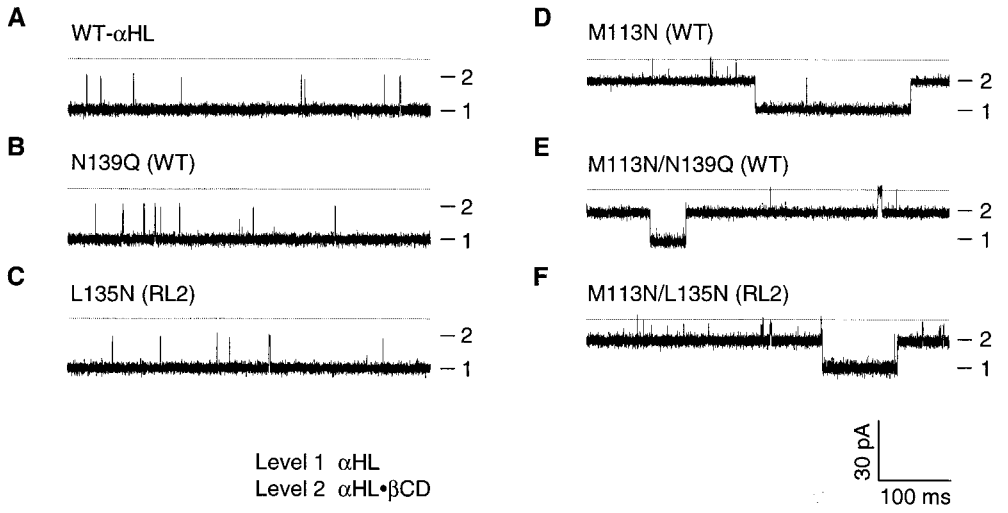

FIGURE 6. Representative current traces from single αHL pores showing blockades by βCD. All traces were recorded under symmetrical conditions in buffer containing 1 M NaCl, 10 mM sodium phosphate, pH 7.5. βCD (40 μM) was present on the trans side of the membrane. (A) WT-αHL, (B) N139Q(WT), (C) L135N(RL2), (D) M113N(WT), (E) M113N/N139Q(WT), and (F) M113N/L135N(RL2). The broken line indicates zero current.

weakly at positive transmembrane potentials than at negative potentials, but binds to others with the opposite dependence on potential (Fig. 2 and Table I). For example, βCD binds to M113E more strongly at +40 mV ($K_d = 3.3 \pm 0.5 \times 10^{-3}$ M) than at −40 mV ($K_d = 1.2 \pm 0.2 \times 10^{-2}$ M), whereas βCD binds to M113R more weakly at +40 mV ($K_d = 1.3 \pm 0.1 \times 10^{-2}$ M) than at −40 mV ($K_d = 1.6 \pm 0.1 \times 10^{-3}$ M).

These data were quantified by using $\beta_{1/K} = \log (K_{d-40}/K_{d+40})$. $\beta_{1/K} > 0$ reflects a stronger affinity for βCD at +40 mV than at −40 mV, and $\beta_{1/K} < 0$, reflects the opposite. Similarly, $\alpha = \log (P_{K+}/P_{Cl-})$ was used as a measure of the charge selectivity of each mutant. Where $\alpha > 0$, a pore is cation selective, and where $\alpha < 0$, a pore is anion selective (Table II). When α and $\beta_{1/K}$ were displayed on a scatter plot, they were seen to be correlated (Fig. 7 A). This means that βCD binds to a cation-selective pore more strongly at positive potentials than at negative potentials, whereas βCD binds to an anion-selective pore more strongly at negative potentials than at positive. Although the effect of mutagenesis on the affinity for βCD was largely reflected in k_{off}, the smaller effect of voltage was manifested in both k_{on} and k_{off} (Fig. 7, B and C).

DISCUSSION

βCD Binds at a Single Site Near Residue 113 in the αHL Pore

Previous work demonstrated that βCD binds within the lumen of the αHL pore (Gu et al., 1999), where it reduces the single-channel conductance (Gu et al., 1999;

TABLE II

Charge Selectivity of Pores and Voltage Dependence of Affinity for βCD

αHL pore	Charge selectivity[a]			Voltage dependence of affinity for βCD	
	V_r	P_{K+}/P_{Cl-}	α	$(1/K_{d+40})/(1/K_{d-40})$	β
	mV				
WT-αHL (pH 5.0)	−15.8	0.34	−0.45	0.25	−0.60
M113R	−13.7	0.39	−0.41	0.11	−0.96
M113K	−11.6	0.46	−0.34	0.16	−0.80
E111N	−7.2	0.63	−0.20	0.13	−0.89
WT-αHL (pH 7.5)	−3.7	0.79	−0.10	0.53	−0.28
M113T	+0.4	1.03	0.01	1.5	0.18
M113V	+1.7	1.12	0.05	2.2	0.34
E111N/K147N	+2.7	1.20	0.08	1.3	0.10
M113P	+3.3	1.24	0.09	2.6	0.42
K147N	+11.5	2.19	0.34	2.9	0.46
WT-αHL (pH 11.0)	+11.9	2.20	0.34	6.6	0.82
M113D	+12.4	2.34	0.37	1.5	0.18
M113E	+13.5	2.54	0.40	3.6	0.56

[a]The reversal potential (V_r) was determined using 1,000 mM KCl (cis) and 200 mM KCl (trans). The charge selectivity (P_{K+}/P_{Cl-}) was calculated by using the GHK equation as described previously (Gu et al., 2000). $\alpha = \log (P_{K+}/P_{Cl-})$, $\beta = \log (K_{d-40}/K_{d+40})$.

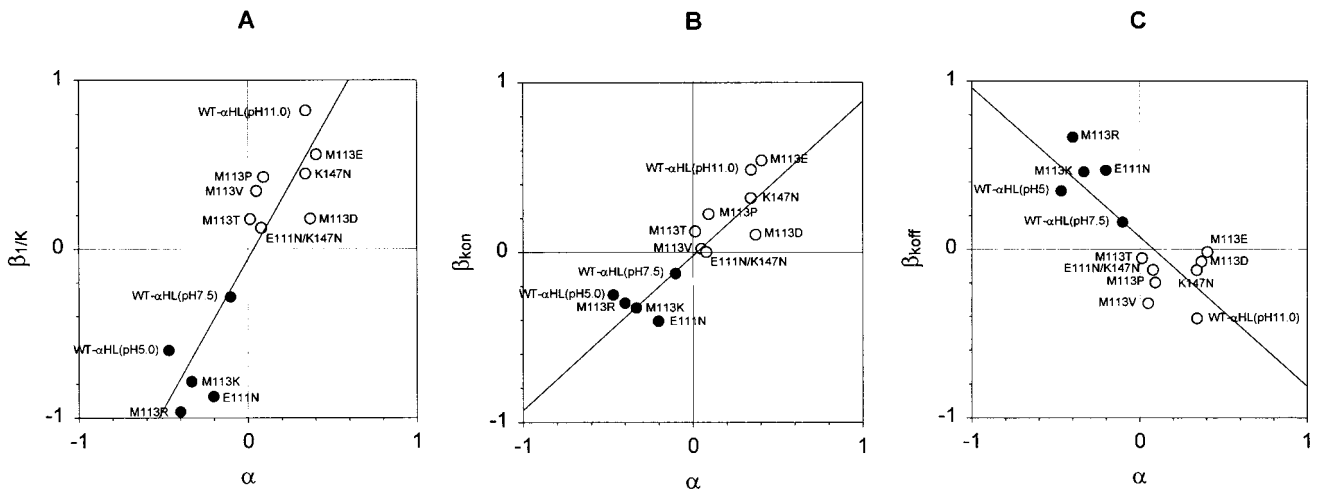

FIGURE 7. Relationships of the voltage dependence of kinetic constants for the interaction of αHL and βCD, and the charge selectivity of the pore. (A) Plot of $\beta_{1/K}$ versus α, where $\beta_{1/K} = \log[(1/K_{d+40})/(1/K_{d-40})] = \log(K_{d-40}/K_{d+40})$ for the mutants in Table II. $\beta_{1/K} > 0$ reflects a stronger affinity at +40 mV than −40 mV, and $\beta_{1/K} < 0$, the opposite. $\alpha = \log(P_{K+}/P_{Cl-})$, a measure of the charge selectivity of each mutant. Where $\alpha > 0$, a pore is cation selective, and where $\alpha < 0$, a pore is anion selective. A line was fitted to the data by linear regression. The correlation coefficient is $R^2 = 0.80$. (B) Plot of β_{kon} versus α, where $\beta_{kon} = \log(k_{on+40}/k_{on-40})$. $R^2 = 0.79$. (C) Plot of β_{koff} versus α, where $\beta_{koff} = \log(k_{off+40}/k_{off-40})$. $R^2 = 0.77$.

Gu and Bayley, 2000), alters ion selectivity (Gu et al., 2000) and acts as a blocker site for various small organic molecules (Gu et al., 1999, 2001). Mutagenesis experiments implied that βCD binds in the vicinity of residue 113. The seven Met-113 side chains in the WT pore project into the lumen of the transmembrane β barrel near its cis end (Fig. 1 A). When the Met-113 residues are replaced with Asn, in M113N, βCD binds 4.4×10^4 times more tightly (Gu et al., 1999, 2001).

The present work, in which all possible natural amino acid substitutions at position 113 were examined and six were found to bind βCD tightly (Table I and Fig. 4), supports the idea that βCD binds at or near residue 113. The variation in the affinity of βCD (K_d) for the mutants at 113 spans a range of about five orders of magnitude, far greater than the roughly two orders observed for βCD and WT-αHL when pH and transmembrane potential were varied (Gu and Bayley, 2000). Further, mutations at positions in the β barrel other than 113, notably 135 and 139, have little effect on the interaction with βCD. WT-αHL (Leu-135, Asn-139), N139Q(WT) (Leu-135, Gln-139), and L135N(RL2) (Asn-135, Gln-139) all share Met-113 and all bind βCD weakly. M113N(WT), M113N/N139Q(WT), and M113N/L135N(RL2) all share Asn-113 and all bind βCD strongly. Similarly, the three pores with Met-113, show conductance blockades by βCD in the range of 37–40%, whereas the three pores with Asn-113 have blockades in the range of 43–46%.

We cannot rule out the possibility that βCD binds at a site removed from position 113 and that mutations at 113 induce conformational changes that affect the binding site. Indeed, the existence of two distinct classes of binding mutants (see next section) is suggestive of low and high affinity states. However, because a second cyclodextrin-binding site can be engineered nearer the trans entrance of the β barrel (Gu et al., 2001) and because βCD cannot bind from the cis side, there are few options for the location of the site under consideration here other than near, but not necessarily in contact with, residue 113. Obviously, additional support for the location of the βCD site through structural studies would be most welcome.

The exact location aside, several arguments suggest that βCD binds at a single site, rather than multiple sites, within the lumen of each αHL mutant. First, for each mutant, there is only one major conductance state that can be assigned to αHL•βCD. Second, there is no additional noise associated with the αHL•βCD state, suggesting that the rather rigid βCD molecule is firmly held at the binding site (Fig. 2). Third, for each mutant, whether binding is strong or weak, the dwell time histograms for τ_{off} and τ_{on} can be fitted to single exponentials (*Supplemental Material*), which is consistent with simple bimolecular kinetics for the interaction of βCD with αHL.

The K_d Values for βCD and Met-113 Replacement Mutants Fall into Two Major Classes

The K_d values for βCD and the Met-113 mutants of αHL fall into two classes: class 1, tight binding mutants, mean $K_d = 6.8 \times 10^{-7}$ M; and class 2, weak binding mutants, mean $K_d = 4.1 \times 10^{-3}$ M. The major determinant of whether a mutant falls into class 1 or class 2 is the dissociation rate constant (k_{off}), values of which fall into the same two classes (Fig. 4). The association rate constant (k_{on}) is hardly changed by mutagenesis (Fig. 4),

suggesting that it may reflect transfer of βCD through the entrance to the pore, which would be expected to be little affected by mutations at position 113. The nature of the mutations that cause tight binding do not fall into an easily recognizable group. However, patterns do appear when the data are examined in detail. For example, whereas M113N and M113D fall into class 1, mutants with homologous substitutions, M113Q and M113E, are in class 2. The one mutant in class 1 with a nonaromatic hydrophobic side chain, M113V, is also the smallest of its kind. Mutants with aromatic substitutions, except the bulky tryptophan, are tight binding. As mentioned above, the existence of two distinct classes of binding mutants is suggestive of low and high affinity states of αHL for βCD. However, this would require a conformational change that is not readily detected in measurements of primary electrical properties, such as single-channel conductance (Fig. 5).

The Interaction of βCD with αHL Is Voltage Dependent and Correlated with the Charge Selectivity of the Mutant Pores

The interaction of βCD with the WT-αHL pore is voltage- and pH-dependent (Gu and Bayley, 2000). At low pH values, βCD (trans) binds more tightly at negative potentials; at high pH values, βCD binds more tightly at positive potentials. Because βCD is a neutral molecule, Woodhull's mechanism for the voltage-dependent binding of a charged blocker was ruled out. Further, because the dissociation rate constant of βCD from its binding site varies continuously with voltage, a mechanism involving the voltage-dependent interconversion of two different states was also discounted. Instead, a continuous change in the free energy of αHL (and/or αHL•βCD) as a function of the membrane potential was postulated (Gu and Bayley, 2000). Voltage-dependent block by neutral molecules has been observed in other systems, but it has not been investigated in detail (Bezrukov et al., 2000).

Like the manipulation of pH, mutagenesis provides another way to change the charge distribution in a protein. In this work, we found that negative substituents at position 113 favor the binding of βCD at positive potentials, whereas positive substituents favor binding at negative potentials (Table II). It is possible that the charge status of residue 113 can determine the affinity of the pore for βCD in the same way that unidentified charged groups do in WT-αHL (Gu and Bayley, 2000). Therefore, an effect of membrane potential on the structure of the pore, as proposed for the pH-dependent properties of WT-αHL (Gu and Bayley, 2000), is also a reasonable explanation for the effects of mutagenesis.

However, the mutagenesis experiments prompt a second possible explanation. The affinity of βCD is correlated with the charge selectivity of the pore, which in αHL is modulated in a predictable manner by the charge at position 113 (Table II). For example, M113K with seven more positive charges than WT-αHL, is more anion selective than WT-αHL, whereas M113E with seven additional negative charges is cation selective. The anion-selective mutants bind βCD, applied from the trans chamber, more tightly at positive applied potentials, whereas the cation-selective mutants bind βCD more tightly at negative potentials (Fig. 7). Just as in the case of pH (Gu and Bayley, 2000), both k_{on} and k_{off} are affected (Fig. 7). Consistent with these data, pH also alters the charge selectivity of the αHL pore (Table II; Krasilnikov et al., 1997). For example, αHL is weakly anion selective at pH 7.5 (P_{K^+}/P_{Cl^-} = 0.77), more anion selective at pH 5.0 (P_{K^+}/P_{Cl^-} = 0.34), and cation selective at pH 11.0 (P_{K^+}/P_{Cl^-} = 2.2). Again, the voltage dependence of the affinity for βCD is correlated with charge selectivity (Table II).

These results show that βCD binding is favored when association occurs in the direction of the net movement of ions and dissociation occurs against the net ion flow. For example, in the case of M113E, a cation-selective channel, net ion flow is from trans to cis in a positive-applied potential, and βCD binding from the trans side of the membrane is enhanced under these conditions. Thus, the second possible explanation is that the βCD molecules move into the pore carried by water flow induced by ion movement—an electroosmotic effect (Katchalsky and Curran, 1965). Because the main barrier to reaching the binding site is entry into the β barrel, it is likely that the water flow would cause accumulation or depletion of the βCD at the trans entrance compared with the bulk concentration and, hence, promote or impede binding.

Water flow caused by electroosmosis is considerable. Applying various simplifications, water flow in a charge-selective pore is given by (Katchalsky and Curran, 1965):

$$J = \frac{RT}{D}\frac{r^2}{8\eta F} I,$$

where D is the diffusion coefficient of the mobile ion; r is the radius of pore; η is the viscosity of water; I is the current flow through pore; and R, T, and F have their usual meanings. At a current of 20 pA, J $\sim 10^9$ s^{-1}. Because 20 pA in a charge-selective pore corresponds to the transport of 1.25×10^8 ions s^{-1}, approximately eight water molecules are transported for each ion that moves through the pore. This is in keeping with experimental findings. For example, in the case of a single cation-selective nafion-filled pore in mica of ~50 μm in radius, ~10 water molecules flow per Na^+ ion transported (Bath et al., 1998, 2000). In the same experiments, neutral organic molecules were shown to move with the water. For example, in the case of 0.2 M hydroquinone, about one molecule was transported for every 1,000 water molecules. For a 40-μM solute, one mole-

cule would move with every 5×10^6 waters. Therefore, if the water flow were $\sim 10^9$ s^{-1} (see above), this would result in an appreciable concentration of βCD at the trans entrance.

To further examine the likelihood of an electroosmotic effect, the mutant E111N/K147N was studied. E111N/K147N is a weakly cation-selective pore ($P_{K^+}/P_{Cl^-} = 1.20$). As expected, βCD applied from the trans chamber binds to E111N/K147N more strongly at positive than at negative potentials ($\beta_{1/K} = 0.10$). In most cases, βCD binds to αHL pores only from the trans side of the bilayer. However, in the case of E111N/K147N, βCD can also bind from the cis side and in this case, the voltage dependency was reversed ($\beta_{1/K} = -0.15$). Although this result is available only for a weakly ion-selective pore, it is in keeping with an electroosmotic mechanism, as opposed to an effect of voltage on the protein. The effects of voltage are also independent of whether a mutant is in class 1 or class 2, and this also favors an electroosmotic mechanism. Otherwise, the effects of voltage would have to be similar on both the conformation of class 1 and that of class 2.

In conclusion, we have shown that long residence times for the noncovalent molecular adapter βCD within the lumen of the αHL pore can be achieved at neutral pH by mutagenesis at position 113. For example, the mean residence time (τ_{off}) for βCD bound to M113N at −40 mV is 27 s. In addition to the greatly enhanced affinity of the class 1 mutants, which most likely arises from alterations of the binding site for βCD in the vicinity of residue 113, the binding can be further enhanced by a voltage-dependent mechanism that may originate in an electroosmotic effect. The latter explanation requires verification through more detailed study. The improved residence times for βCD will contribute to our ability to build nanostructures from the αHL pore (Gu et al., 2001) and to use it as a component of stochastic sensors (Bayley and Cremer, 2001).

We thank Orit Braha, Alan Finkelstein, Chuck Martin, Liviu Movileanu, and the reviewers for their remarks.

This paper was supported by the US Department of Energy, the National Institutes of Health, the Office of Naval Research (MURI 1999), and the Texas Advanced Technology Program.

Submitted: 6 July 2001
Revised: 7 September 2001
Accepted: 11 September 2001

REFERENCES

Bath, B.R., R.D. Lee, H.S. White, and E.R. Scott. 1998. Imaging molecular transport in porous membranes. Observation and analysis of electroosmotic flow in individual pores using the scanning electrochemical microscope. *Anal. Chem.* 70:1047–1058.

Bath, B.R., H.S. White, and E.R. Scott. 2000. Electrically facilitated molecular transport. Analysis of the relative contributions of diffusion, migration, and electroosmosis to solute transport in an ion-exchange membrane. *Anal. Chem.* 72:433–442.

Bayley, H. 1995. Pore-forming proteins with built-in triggers and switches. *Bioorg. Chem.* 23:340–345.

Bayley, H. 1997. Building a door into cells. *Sci. Am.* 277:62–67.

Bayley, H. 1999. Designed membrane channels and pores. *Curr. Opin. Biotechnol.* 10:94–103.

Bayley, H., O. Braha, and L.-Q. Gu. 2000. Stochastic sensing with protein pores. *Adv. Mater.* 12:139–142.

Bayley, H., and P.S. Cremer. 2001. Stochastic sensors inspired by biology. *Nature.* 413:226–230.

Bezrukov, S.M., L. Kullman, and M. Winterhalter. 2000. Probing sugar translocation through maltoporin at the single channel level. *FEBS Lett.* 476:224–228.

Bhakdi, S., R. Füssle, and J. Tranum-Jensen. 1981. Staphylococcal α-toxin: oligomerization of hydrophilic monomers to form amphiphilic hexamers induced through contact with deoxycholate micelles. *Proc. Natl. Acad. Sci. USA.* 78:5475–5479.

Braha, O., B. Walker, S. Cheley, J.J. Kasianowicz, L. Song, J.E. Gouaux, and H. Bayley. 1997. Designed protein pores as components for biosensors. *Chem. Biol.* 4:497–505.

Braha, O., L.-Q. Gu, L. Zhou, X. Lu, S. Cheley, and H. Bayley. 2000. Simultaneous stochastic sensing of divalent metal ions. *Nat. Biotechnol.* 17:1005–1007.

Cheley, S., M.S. Malghani, L. Song, M. Hobaugh, J.E. Gouaux, J. Yang, and H. Bayley. 1997. Spontaneous oligomerization of a staphylococcal a-hemolysin conformationally constrained by removal of residues that form the transmembrane b barrel. *Protein Eng.* 10:1433–1443.

Cheley, S., O. Braha, X. Lu, S. Conlan, and H. Bayley. 1999. A functional protein pore with a "retro" transmembrane domain. *Protein Sci.* 8:1257–1267.

Creighton, T.E. 1993. Proteins: Structures and Molecular Properties. Freeman, New York. 507 p.

D'Souza, V.T., and K.B. Lipkowitz. 1998. Cyclodextrins. *Chem. Rev.* 98:1741–2076.

Eroglu, A., M.J. Russo, R. Bieganski, A. Fowler, S. Cheley, H. Bayley, and M. Toner. 2000. Intracellular trehalose improves the survival of cryopreserved mammalian cells. *Nat. Biotechnol.* 18:163–167.

Füssle, R., S. Bhakdi, A. Sziegoleit, J. Tranum-Jensen, T. Kranz, and H.-J. Wellensiek. 1981. On the mechanism of membrane damage by *Staphylococcus aureus* α-toxin. *J. Cell Biol.* 91:83–94.

Gu, L.-Q., and H. Bayley. 2000. Interaction of the non-covalent molecular adapter, β-cyclodextrin, with the staphylococcal α-hemolysin pore. *Biophys. J.* 79:1967–1975.

Gu, L.-Q., O. Braha, S. Conlan, S. Cheley, and H. Bayley. 1999. Stochastic sensing of organic analytes by a pore-forming protein containing a molecular adapter. *Nature.* 398:686–690.

Gu, L.-Q., M. Dalla Serra, J.B. Vincent, G. Vigh, S. Cheley, O. Braha, and H. Bayley. 2000. Reversal of charge selectivity in transmembrane protein pores by using non-covalent molecular adapters. *Proc. Natl. Acad. Sci. USA.* 97:3959–3964.

Gu, L.-Q., S. Cheley, and H. Bayley. 2001. Capture of a single molecule in a nanocavity. *Science.* 291:636–640.

Howorka, S., S. Cheley, and H. Bayley. 2001a. Sequence-specific detection of individual DNA strands using engineered nanopores. *Nat. Biotechnol.* 19:636–639.

Howorka, S., L. Movileanu, O. Braha, and H. Bayley. 2001b. Kinetics of duplex formation for individual DNA strands within a single protein nanopore. *Proc. Natl. Acad. Sci. USA.* In press.

Kasianowicz, J.J., E. Brandin, D. Branton, and D.W. DeAm. 1996. Characterization of individual polynucleotide molecules using a membrane channel. *Proc. Natl. Acad. Sci. USA.* 93:13770–13773.

Katchalsky, A., and P.F. Curran. 1965. Nonequilibrium Thermodynamics in Biophysics. Harvard University Press, Cambridge, MA. 248 p.

Krasilnikov, O.V., M.-F.P. Capistrano, L.N. Yuldasheva, and R.A. Nogueira. 1997. Influence of Cys-130 *S. aureus* alpha-toxin on

planar lipid bilayer and erythrocyte membranes. *J. Membr. Biol.* 156:157–172.

Montal, M., and P. Mueller. 1972. Formation of bimolecular membranes from lipid monolayers and study of their electrical properties. *Proc. Natl. Acad. Sci. USA.* 69:3561–3566.

Movileanu, L., S. Howorka, O. Braha, and H. Bayley. 2000. Detecting protein analytes that modulate transmembrane movement of a polymer chain within a single protein pore. *Nat. Biotechnol.* 18: 1091–1095.

Otto-Bruc, A.E., R.N. Fariss, J.P. Van Hooser, and K. Palczewski. 1998. Phosphorylation of photolyzed rhodopsin is calcium-insensitive in retina permeabilized by α-toxin. *Proc. Natl. Acad. Sci. USA.* 95:15014–15019.

Panchal, R.G., E. Cusack, S. Cheley, and H. Bayley. 1996. Tumor protease-activated, pore-forming toxins from a combinatorial library. *Nat. Biotechnol.* 14:852–856.

Russo, M.J., H. Bayley, and M. Toner. 1997. Reversible permeabilization of plasma membranes with an engineered switchable pore. *Nat. Biotechnol.* 15:278–282.

Sanchez-Quesada, J., M.R. Ghadiri, H. Bayley, and O. Braha. 2000. Cyclic peptides as molecular adapters for a pore-forming protein. *J. Am. Chem. Soc.* 122:11758–11766.

Song, L., M.R. Hobaugh, C. Shustak, S. Cheley, H. Bayley, and J.E. Gouaux. 1996. Structure of staphylococcal α-hemolysin, a heptameric transmembrane pore. *Science.* 274:1859–1865.

Walker, B.J., and H. Bayley. 1994. A pore-forming protein with a protease-activated trigger. *Prot. Eng.* 7:91–97.

Walker, B.J., M. Krishnasastry, L. Zorn, J.J. Kasianowicz, and H. Bayley. 1992. Functional expression of the α-hemolysin of *Staphylococcus aureus* in intact *Escherichia coli* and in cell lysates. *J. Biol. Chem.* 267:10902–10909.